

Impact of layer defects in ferroelectric thin films

This article has been downloaded from IOPscience. Please scroll down to see the full text article.

2005 J. Phys.: Condens. Matter 17 4687

(<http://iopscience.iop.org/0953-8984/17/29/010>)

View [the table of contents for this issue](#), or go to the [journal homepage](#) for more

Download details:

IP Address: 129.252.86.83

The article was downloaded on 28/05/2010 at 05:38

Please note that [terms and conditions apply](#).

Impact of layer defects in ferroelectric thin films

J M Wesselinowa¹, S Trimper² and K Zabrocki²

¹ Department of Physics, University of Sofia, Boulevard J Bouchier 5, 1164 Sofia, Bulgaria

² Fachbereich Physik, Martin-Luther-Universität, D-06099 Halle, Germany

E-mail: julia@phys.uni-sofia.bg and trimper@physik.uni-halle.de

Received 14 April 2005, in final form 13 June 2005

Published 8 July 2005

Online at stacks.iop.org/JPhysCM/17/4687

Abstract

Based on a modified Ising model in a transverse field we demonstrate that defect layers in ferroelectric thin films, such as layers with impurities, vacancies or dislocations, are able to induce a strong increase or decrease of the polarization depending on the variation of the exchange interaction within the defect layers. A Green function technique enables us to calculate the polarization, the excitation energy and the critical temperature of the material with structural defects. Numerically we find the polarization as a function of temperature, film thickness and the interaction strengths between the layers. The theoretical results are in reasonable accordance with experimental data of different ferroelectric thin films.

1. Introduction

Defects in crystals influence significantly the physical properties of almost all materials. The fact that perovskite oxides such as $\text{Pb}(\text{Zr}, \text{Ti})\text{O}_3$ (PZT) develop planar ordered arrays of defects has a long history. The first observation is due to Grenier *et al* [1], as well as Becerro *et al* [2] and Steinsvik *et al* [3]. The observed superlattice structure can significantly affect the phase transition temperature, the dielectric properties and the transport behaviour. Thus all the conductivity contributions increase with increasing iron content in $\text{SrTi}_{1-x}\text{Fe}_x\text{O}_{3-y}$ [3]. The role of planar effects on ferroelectric properties, such as fatigue in PZT, was first examined in [4], and later also in [5] and [6]. As a consequence of the strong influence of defects in dielectric properties a kind of defect engineering has been developed as a part of modern semiconductor technology. Based on the extensive research before on ferroelectrics (FEs), especially on FE thin films, and due to their suitability for applications in nonvolatile FE random access memories (FERAMs) [7], there is a further increasing interest in studying defects and their related FE strain fields, in particular in low dimensional systems [8]. A broad variety of defects have been implemented and analysed mainly in ABO_3 -type FEs, such as BaTiO_3 , PZT [8–11], and bismuth layer-structured FEs, such as $\text{Bi}_4\text{Ti}_3\text{O}_{12}$ (BTO) [12–15] as well as $\text{SrBi}_2\text{Ta}_2\text{O}_9$ (SBT) [16–18]. To control the polarization and the piezoelectric properties,

PZT is often modified by various elements of lower valency (K, Mn, Fe) and higher valency (La, Nb, Ta) cations. The modified PZTs are generally classified into the two categories named ‘hard’ and ‘soft’ ones [19]. The substitution of lower valency cations, compared to the constituent ions, leads to oxide vacancies which induces a soft FE behaviour, whereas higher valency substitution gives rise to cation vacancies offering a hard FE behaviour. In contrast to the hard FEs, the soft FEs are characterized by a lower coercive field strength E_c , lower remanent polarization σ_r and higher hysteresis losses. The different FE properties are generally originated by the occurrence of defects. In materials in confined dimensions, the influence of defects can be even more pronounced due to the enhanced relative volume of the ‘defective’ regions [11].

For applications the thin ferroelectric film should reveal large remanent polarizations, low coercive fields, and fatigue-free properties. PZT and SBT have been widely investigated as appropriate material in FERAMs. Otherwise the poor fatigue characteristics [4] and the small remanent polarization are viewed as the major barrier for their applications.

BTO is a promising alternative to PZT, because of its large spontaneous polarization along the a -axis. Recently, it was reported that the substitution of small amounts of impurities, such as Sm and Nd for Bi and V, W and Nb for Ti, in the pseudoperovskite $[(\text{Bi}_2\text{Ti}_3\text{O}_{10})^{2-}]$ layers of BTO is effective for lowering the leakage current and enhancing the remanent polarization [13–15]. Noguchi *et al* [16] reported the control of FE properties in Sr-site-modified SBT bulk ceramics, in which the Sr-site was partially substituted by La atoms and showed a lower coercive field than the original material; however, the remanent polarization was also decreased in this material. On the other hand, several reports have revealed that the σ_r value is enhanced in Sr-deficient and Bi-excess SBT films because of the substitution of excess Bi atoms in the Sr site [20, 21]. However, E_c also increases in these films. Since the ionic radius of the La ion is almost the same as that of the Bi ion, the electronegativity is also important for controlling the FE properties in the site-engineering technique. In fact, the electronegativity of a Bi ion is much higher than that of a La ion. A similar effect was obtained in Sr-deficient and Pr-substituted SBT films [17].

PZT films are considered the most promising candidates for applications in microelectromechanical systems (MEMS) since they have large piezoelectric coefficients and electromechanical coupling coefficients. As known from bulk ceramics, the piezoelectric and dielectric properties vary substantially with the composition (Zr to Ti ratio). While the bulk PZT ceramics have been well investigated, there is still a lack of understanding the piezoelectric and dielectric properties of PZT thin films, particularly as a function of composition. With increasing Ti-content, larger remanent polarization and higher coercive voltage are observed [8]. Impact of misfit dislocations on the polarization instability of epitaxial nanostructured FE perovskites (PZT nanoislands) is investigated by Chu *et al* [11]. Their results suggest that misfit engineering is indispensable for obtaining nanostructured FEs with stable polarization. The properties of BaTiO_3 are modified by substituting of tetravalent ions such as Zr^{4+} for Ti sites. This increases the dielectric constant and broadens the sharp temperature dependence of the dielectric constant around the Curie temperature. With the addition of strontium to PbTiO_3 , the phase-transition temperature decreases with the increasing Sr concentration.

The influence of defects on FE phase transitions is one of the key-like topics of modern studies of FEs. The everlasting attention to this topic is related to both the understanding of the basic mechanism in FEs and the above mentioned applications. It is well known that localized spin excitations can arise in FEs and magnetic systems with broken spatial translational symmetry, i.e. due to the presence of boundary surfaces, interfaces, impurities and other defects in the crystal. These localized modes appearing in the above mentioned

structures are experimentally observed using the neutron and Raman scattering [22, 23], or, more recently, far infrared absorption [24]. The Green function theories have been extensively employed to describe these modes in semi-infinite transverse Ising models [25] and FE thin films [26]. In addition to bulk spin waves there may be localized modes associated with the impurity layer [25] and with the surface [26]. A transfer matrix formalism is applied to study a semi-infinite Heisenberg ferromagnetic superlattice with a surface cell and an impurity cell at arbitrary distance from the surface [27]. The occurrence of localized modes associated with the impurity cell is demonstrated sufficiently. In the dielectric continuum approximation, Zhang *et al* [28] investigated the effect of different kinds of coupling to the localized interface optical-phonon modes in two coupled semi-infinite N -constituent superlattices with a structural defect layer. The influence of molecular impurity ions on FE phase transitions is studied by Vikhin and Maksimova [29] using the phenomenological Landau theory. It is shown that molecular impurity ions with charge transfer–local vibration degrees of freedom, which bi-linearly interact with the FE order parameter, can induce rather strong increase of the critical temperature of FE phase transition at reasonable concentrations of molecular impurities. This could be topical, for instance, for the KDP-MnO₄ case. Using a combination of first-principles and effective-Hamiltonian approaches, Dieguez *et al* [30] obtained a phase diagram in temperature and misfit strain in epitaxial BaTiO₃ that is qualitatively different from that reported by Pertsev *et al* [31]. In particular, in [30] is found a region of ‘ r phase’ at low temperature where Pertsev *et al* have reported an ‘ ac phase’.

Most of the published papers consider the defects’ influence on the spin excitations. A first attempt to find out the influence of defects on the polarization of FE thin films is elucidated by Alpay *et al* [32, 33]. A thermodynamic analysis has been carried out to investigate the role of dislocations in FE materials. Due to the coupling of the stress field of the dislocation and the polarization, there is expected a drastic variation of the polarization near to the dislocation. The compressive regions enhance the polarization and increase Curie temperature whereas tensile stresses decrease polarization with a commensurate drop in the Curie temperature [32, 33]. But actually, the dependence of the polarization and the Curie temperature on defects in FE thin films is not so intensively studied theoretically. Therefore, it is the aim of the present paper to investigate the polarization of FE thin films with defect layers in more detail and based on a microscopic approach. Recently, it was established that the phase transition temperature T_c does not increase in very thin films, down to about 2.4 nm. This fact is attributed to oxygen vacancy gradients as shown theoretically in [34, 35] and experimentally [36, 37]. Notice that there is a very recent result [38] where local ferroelectric distortions and the temperature–misfit strain phase diagram in ultra-thin films are calculated from first principles.

Whereas the modelling in [34, 35] is essentially based on a mesoscopic approach in the framework of a Landau theory in our paper we use a more microscopic approach to study the influence of defect layers. With this aim an Ising model in a transverse field with additional defect layers is considered. Using Green function methods we calculate the spin-wave energies, the polarization and the phase transition temperature for an FE thin film with different structural defect layers. The numerical results are compared with those of bulk materials and with thin films without defect layers. Different to the recent paper [38], the inclusion of elastic degrees of freedom is not considered here. This will be shifted to a forthcoming work.

2. The model and the matrix Green function

Let us consider a three-dimensional ferroelectric system on a simple cubic lattice composed of N layers in the z -direction. The layers are numbered by $n = 1, \dots, N$, where the layers $n = 1$ and $n = N$ represent the two surfaces of the system. The bulk is established by the

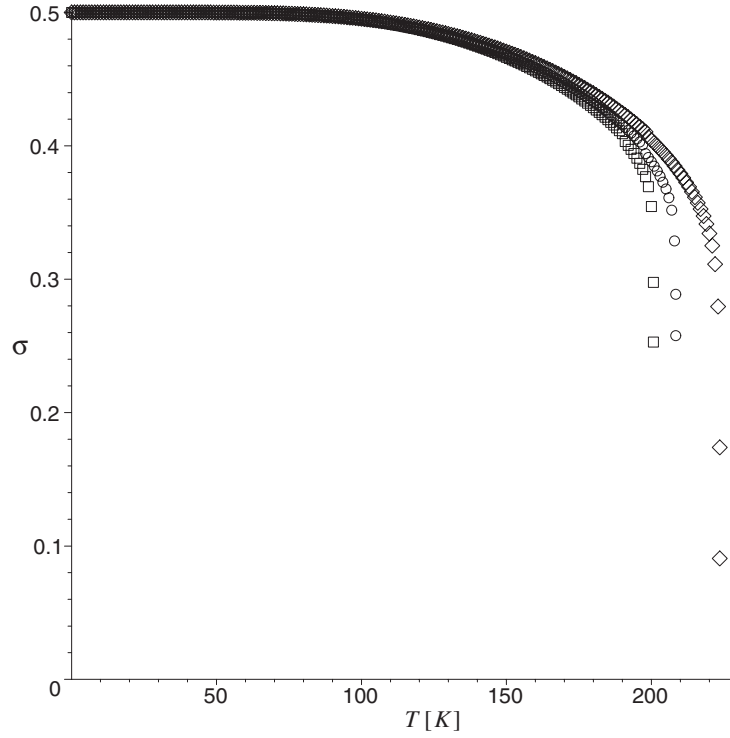


Figure 1. Temperature dependence of the polarization σ for an FE thin film with $J_b = 495$ K, $\Omega_b = 20$ K, $J_s = 900$ K, $\Omega_s = \Omega_b$, $N = 9$ and different J_d -values: (1) $J_d = 300$ K, $T_c = 201$ K (\square), (2) 495 K, $T_c = 208$ K (\circ), (3) 1000 K, $T_c = 224$ K (\diamond).

remaining $(N - 2)$ layers. The specific surface effects are included by additional coupling parameters between bulk and surface layers. In particular, we start with the Hamiltonian of the Ising model in a transverse field which includes both bulk and surface properties.

$$H = -\frac{1}{2} \sum_{ij} J_{ij} S_i^z S_j^z - \Omega_b \sum_{i \in b} S_i^x - \Omega_s \sum_{i \in s} S_i^x, \quad (1)$$

where S^x and S^z are components of spin- $\frac{1}{2}$ operators, and Ω_b and Ω_s represent transverse fields in the bulk and surface layers, and the sums are over the internal and surface lattice points, respectively. J_{ij} is an exchange interaction between spins at nearest-neighbour sites i and j , and $J_{ij} = J_s$ between spins on the surface layer, otherwise the interaction in the bulk material is denoted by J_b . Additionally, we assume that one or more of the layers can be defected; the interaction strength of these defect layers is characterized by J_d and the corresponding transverse field by Ω_d . Because the ordered phase is determined by $\langle S^x \rangle \neq 0$ and $\langle S^z \rangle \neq 0$, it is appropriate to introduce a new coordinate system rotated by an angle θ in the x - y plane [26]. The rotation angle θ is defined by the requirement $\langle S^{x'} \rangle = 0$, where $S^{x'}$ is the spin component in the rotated coordinate system. In our approximation the angle θ is calculated below; see equation (5).

The retarded Green function to be calculated is defined as

$$G_{ij}(t) = \langle \langle S_i^+(t); S_j^-(0) \rangle \rangle, \quad (2)$$

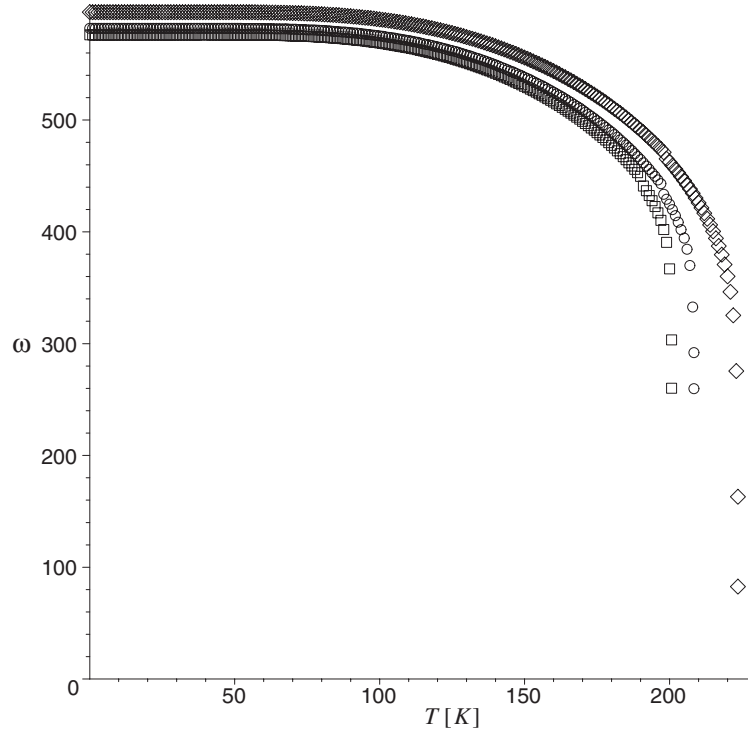


Figure 2. Temperature dependence of the spin-wave energy ω (cm^{-1}) for an FE thin film with $J_b = 495$ K, $\Omega_b = 20$ K, $J_s = 900$ K, $\Omega_s = \Omega_b$, $N = 9$ and different J_d -values: (1) $J_d = 300$ K (\square), (2) 495 K (\circ), (3) 1000 K (\diamond).

where S^+ and S^- are the spin- $\frac{1}{2}$ operators in the rotated system. On introducing the two-dimensional Fourier transform $\bar{G}_{n_i n_j}(\mathbf{k}_{\parallel}, \omega)$, one has the following form:

$$\langle\langle S_i^+; S_j^- \rangle\rangle_{\omega} = \frac{\sigma}{N'} \sum_{\mathbf{k}_{\parallel}} \exp(i\mathbf{k}_{\parallel}(\mathbf{r}_i - \mathbf{r}_j)) G_{n_i n_j}(\mathbf{k}_{\parallel}, \omega), \quad (3)$$

where N' is the number of sites in any of the lattice planes, \mathbf{r}_i and n_i represent the position vectors of site i and the layer index, respectively, and $\mathbf{k}_{\parallel} = (k_x, k_y)$ is a two-dimensional wavevector parallel to the surface. The summation is taken over the Brillouin zone.

As a result the equation of motion for the Green function in equation (3) of the ferroelectric thin film for $T \leq T_c$ has the following matrix form:

$$\mathbf{H}(\omega) \mathbf{G}(\mathbf{k}_{\parallel}, \omega) = \mathbf{R}, \quad (4)$$

where \mathbf{H} can be expressed as

$$\mathbf{H} = \begin{pmatrix} \omega - V_1 & k_1 & 0 & 0 & 0 & 0 & \dots \\ k_2 & \omega - V_2 & k_2 & 0 & 0 & 0 & \dots \\ 0 & k_3 & \omega - V_3 & k_3 & 0 & 0 & \dots \\ \vdots & \vdots & \vdots & \vdots & \vdots & \vdots & \ddots \\ 0 & 0 & 0 & 0 & 0 & k_N & \omega - V_N \end{pmatrix}$$

with

$$K_n = J_b \sigma_n \sin^2 \theta_n, \quad n = 1, \dots, N,$$

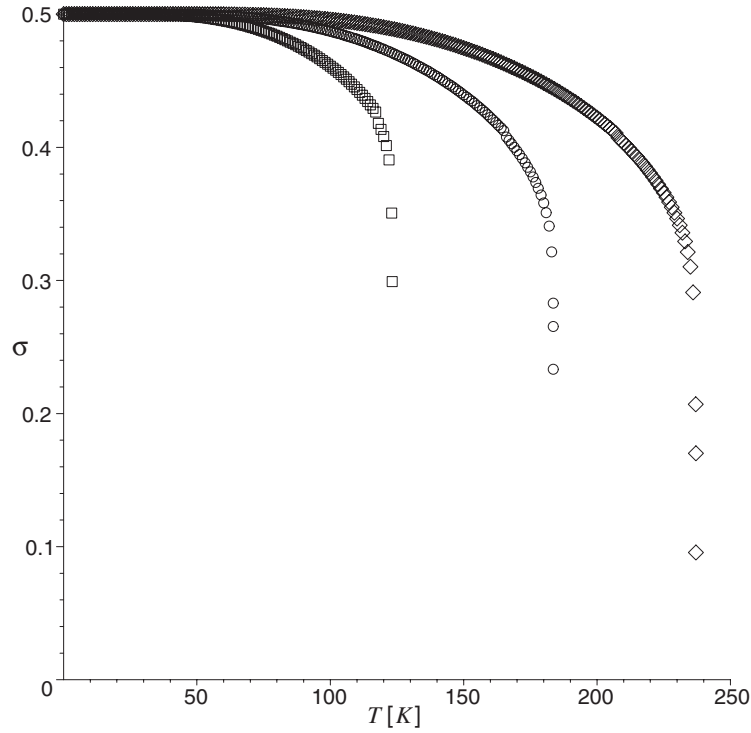


Figure 3. Temperature dependence of the polarization σ for $J_b = 495$ K, $\Omega_b = 20$ K, $J_d = 1000$ K, $\Omega_s = \Omega_b$, $N = 7$ and different J_s -values: (1) $J_s = 200$ K, $T_c = 123$ K (\square), (2) 500 K, $T_c = 184$ K (\circ), (3) 1000 K, $T_c = 237$ K (\diamond).

$$\begin{aligned}
 V_1 &= 2\Omega_s \sin \theta_1 + \frac{1}{2}\sigma_1 J_s \cos^2 \theta_1 - \frac{\sigma_1 J_s}{4} \sin^2 \theta_1 \gamma(\mathbf{k}_{\parallel}) + J_b \sigma_2 \cos^2 \theta_2, \\
 V_2 &= 2\Omega_b \sin \theta_2 + \frac{1}{2}\sigma_2 J_b \cos^2 \theta_2 - \frac{\sigma_2 J_b}{4} \sin^2 \theta_2 \gamma(\mathbf{k}_{\parallel}) + J_s \sigma_1 \cos^2 \theta_2 + J_b \sigma_3 \cos^2 \theta_3, \\
 V_n &= 2\Omega_n \sin \theta_n + \frac{1}{2}\sigma_n J_b \cos^2 \theta_n - \frac{\sigma_n J_n}{4} \sin^2 \theta_n \gamma(\mathbf{k}_{\parallel}) + J_{n-1} \sigma_{n-1} \cos^2 \theta_{n-1} \\
 &\quad + J_{n+1} \sigma_{n+1} \cos^2 \theta_{n+1}, \\
 V_N &= 2\Omega_s \sin \theta_N + \frac{1}{2}\sigma_N J_s \cos^2 \theta_N - \frac{\sigma_N J_s}{4} \sin^2 \theta_N \gamma(\mathbf{k}_{\parallel}) + J_b \sigma_{N-1} \cos^2 \theta_{N-1}, \\
 \gamma(\mathbf{k}_{\parallel}) &= \frac{1}{2}(\cos(k_x a) + \cos(k_y a)).
 \end{aligned}$$

Here we have introduced the notations $J_1 \equiv J_N = J_s$, $J_n = J_b$ for $n = 2, 3, 4, \dots, N-1$, $\Omega_1 = \Omega_N = \Omega_s$, $\Omega_n = \Omega_b$ ($n = 2, 3, 4, \dots, N-1$), $J_0 = J_{N+1} = 0$. The quantity $\sigma(T)$ is the relative polarization in the direction of the mean field and is equal to $2\langle S^z \rangle$. The rotation angle θ is defined by vanishing the anomalous averages $\langle S^{x'} \rangle = \langle S^{y'} \rangle = 0$. We find the following two solution in our generalized Hartree–Fock decoupling approximation:

$$\begin{aligned}
 1. \quad & \cos \theta = 0, \quad \text{i.e. } \theta = \frac{\pi}{2}, \quad \text{if } T \geq T_c; \\
 2. \quad & \sin \theta = \frac{4\Omega}{\sigma J} = \frac{\sigma_c}{\sigma}, \quad \text{if } T \leq T_c.
 \end{aligned} \tag{5}$$

Here the phase transition temperature T_c is defined by the relation $\sigma(T_c) = \sigma_c \equiv 4\Omega/J$. In order to obtain the solutions of the matrix equation (4), we introduce the two-dimensional

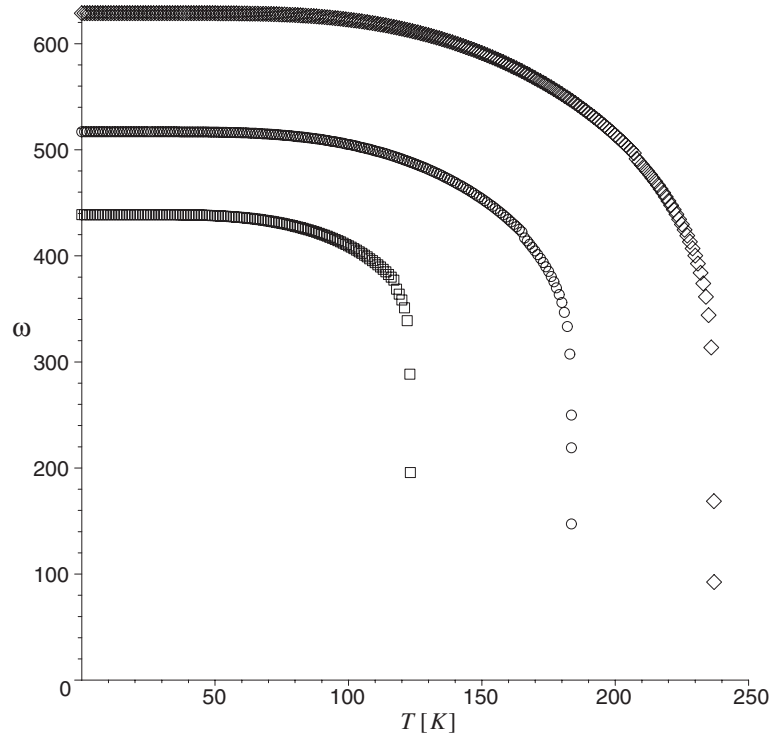


Figure 4. Temperature dependence of the spin-wave energy ω (cm^{-1}) for $J_b = 495$ K, $\Omega_b = 20$ K, $J_d = 1000$ K, $\Omega_s = \Omega_b$, $N = 7$ and different J_s -values: (1) $J_s = 200$ K (\square), (2) 500 K (\circ), (3) 1000 K (\diamond).

column matrices, \mathbf{G}_m and \mathbf{R}_m , where the elements are given by $(\mathbf{G}_n)_m = G_{mn}$ and $(\mathbf{R}_n)_m = \sigma_n \delta_{mn}$, so that equation (4) yields

$$\mathbf{H}(\omega)\mathbf{G}_n = \mathbf{R}_n. \quad (6)$$

From equation (6), $G_{nn}(\omega)$ is obtained as

$$G_{nn}(\omega) = \frac{|H_{nn}(\omega)|}{|H(\omega)|}. \quad (7)$$

The quantity $|H_{nn}(\omega)|$ is the determinant made by replacing the n th column of the determinant $|H(\omega)|$ by R_n . The poles ω_n of the Green function $G_{nn}(\omega)$ can be calculated by solving $|H(\omega)| = 0$.

The relative polarization of the of the n th layer is given by

$$\sigma_n = \left(\frac{\sigma_n J_n}{2N} \sum_{\mathbf{k}_{\parallel}} \frac{1 - 0.5 \sin^2 \theta_n \gamma(\mathbf{k}_{\parallel})}{\omega_n} \coth \frac{\omega_n}{2T} \right)^{-1}. \quad (8)$$

The last equation has to be calculated numerically. Due to the assumption of symmetrical surfaces, there are $\frac{1}{2}N$ layer polarizations, which have to be solved self-consistently. In order to obtain the dependence of the Curie temperature T_C on the film thickness N , we let all σ s be zero in equation (8) and solve the expressions self-consistently.

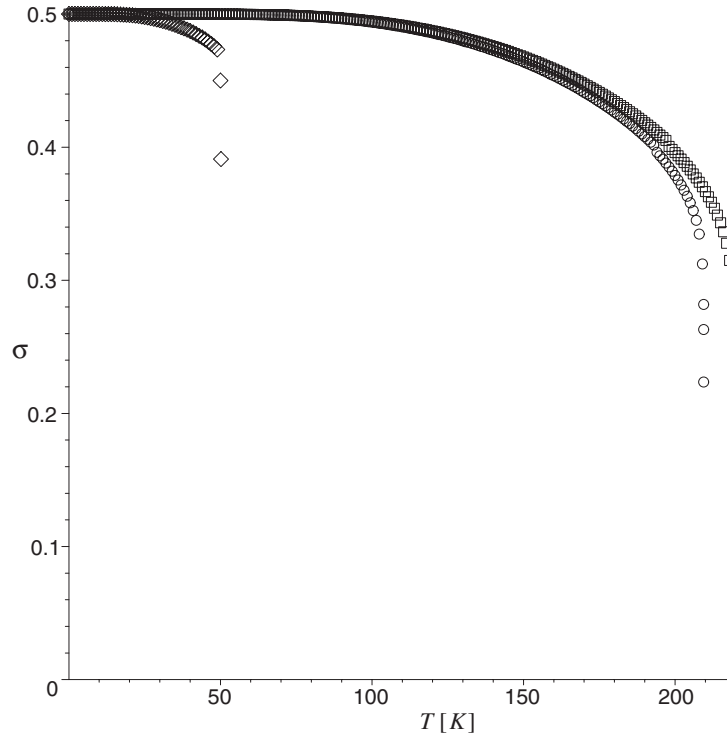


Figure 5. Temperature dependence of the polarization σ for $J_b = 495$ K, $\Omega_b = 20$ K, $J_s = 900$ K, $\Omega_s = \Omega_b$, $N = 7$ and different defect layers: (1) $J_4 = J_b = 495$ K, $T_c = 220$ K (\square), (2) $J_4 = J_d = 200$ K, $T_c = 209$ K (\circ), (3) $J_3 = J_4 = J_5 = J_d = 200$ K, $T_c = 50$ K (\diamond).

3. Numerical results and discussion

In this section we present the numerical results based on our theoretical calculations taking the typical bulk parameter $J_b = 495$ K and $\Omega_b = 20$ K. We have calculated the temperature dependence of the polarization defined by

$$\sigma \equiv \langle S^z \rangle = \frac{1}{N} \sum_n \sigma_n(T) \cos \theta_n,$$

and the spin-wave frequencies of thin films for different values of the exchange interaction constants. One has to solve self-consistently the $\frac{1}{2}N$ coupled equations (8) to obtain the layer polarization from the surface to half of the film (the other half is symmetric due to the assumption of identical surfaces). The numerical results expose some interesting and novel characteristics in the polarization and the spin-wave energies in comparison to the case of FE thin films without defects. To characterize the complete ferroelectric system both quantities, the polarization σ and the spin-wave energy ω , respectively, are averaged over the N layers. The results for film thickness $N = 9$ and different exchange interaction parameters in the defect layers J_d are presented in figures 1 and 2. Let us firstly consider the case where the middle layer is a defect layer. For example, this can be originated by localized vacancies or impurities with smaller radii and larger distances between them in comparison to the host material. It is reasonable to assume that the exchange interaction J_d is smaller than the value of the bulk interaction $J_b = 495$ K and has the value $J_5 = J_d = 300$ K (compare figures 1, 2 curve 1).

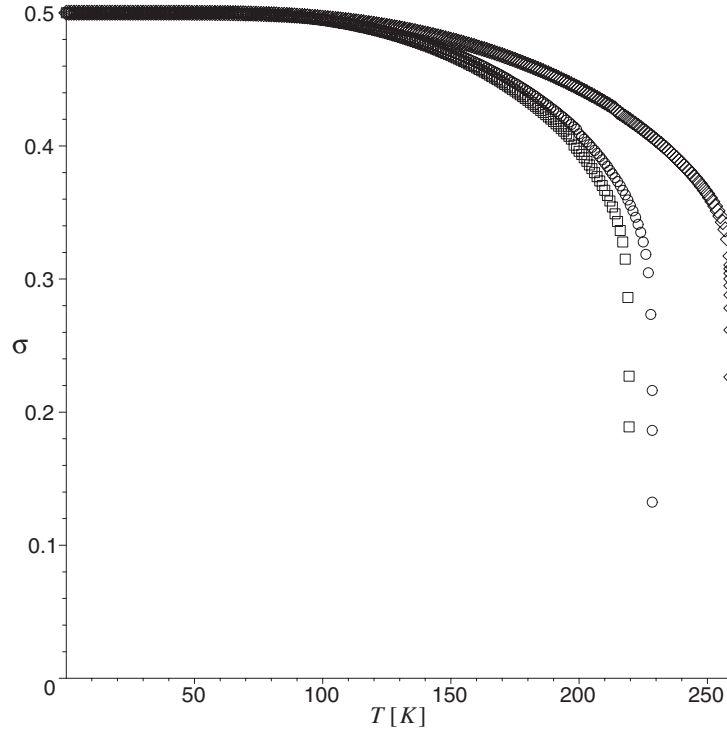


Figure 6. Temperature dependence of the polarization σ for $J_b = 495$ K, $\Omega_b = 20$ K, $J_s = 900$ K, $\Omega_s = \Omega_b$, $N = 7$ and different defect layers: (1) $J_d = J_b = 495$ K, $T_c = 220$ K (\square), (2) $J_d = J_b = 1000$ K, $T_c = 229$ K (\circ), (3) $J_d = J_b = 1000$ K, $T_c = 259$ K (\diamond).

The polarization (respectively the spin-wave energy) is smaller than the case without defects, $J_5 = J_b$ (see figures 1, 2 curve 2). The polarization decreases with increasing temperature to vanish at the critical temperature T_c of the thin film. The critical temperature decreases due to the smaller J_d value. Pontes *et al* [10] carried out dielectric and Raman spectroscopy studies and found that with addition of Sr to PbTiO_3 the phase-transition temperature decreases with the increasing Sr concentration.

For the case where $J_5 = J_d = 1000$ K (figures 1, 2, curve 3), i.e. J_d is larger than the value of the bulk interaction constant J_b (for example when the impurities have a larger radius compared with the constituent ions), the polarization (respectively the spin-wave energy) is larger than the case without defects, $J_5 = J_b$. The T_c of the film is enhanced in comparison to the bulk value without defects due to the presence of larger J_d values. This is the opposite behaviour compared to the case of $J_d = 300$ K, $J_d < J_b$. Of course, in the case of both strong and small J_d values, thin film polarizations tend to the 3D one when n increases, since the excitation spectrum varies from 2D to 3D behaviour with thickness. The second case, where $J_d > J_b$, could explain the experimentally obtained increase in polarization by the substitution of impurities, such as Nd, V, W and Nb in the layers of BTO films [13–15] or by increasing Ca contents in SBT thin films [18].

From figures 1 and 2 one can observe that the polarization, the spin-wave energies and the critical temperature of the FE phase transition are increased or decreased due to different exchange interactions in the defect layers. Our results are in qualitative agreement with the experimental data of Noguchi *et al* [21]. They have studied SBT films ($T_c = 295^\circ\text{C}$) by

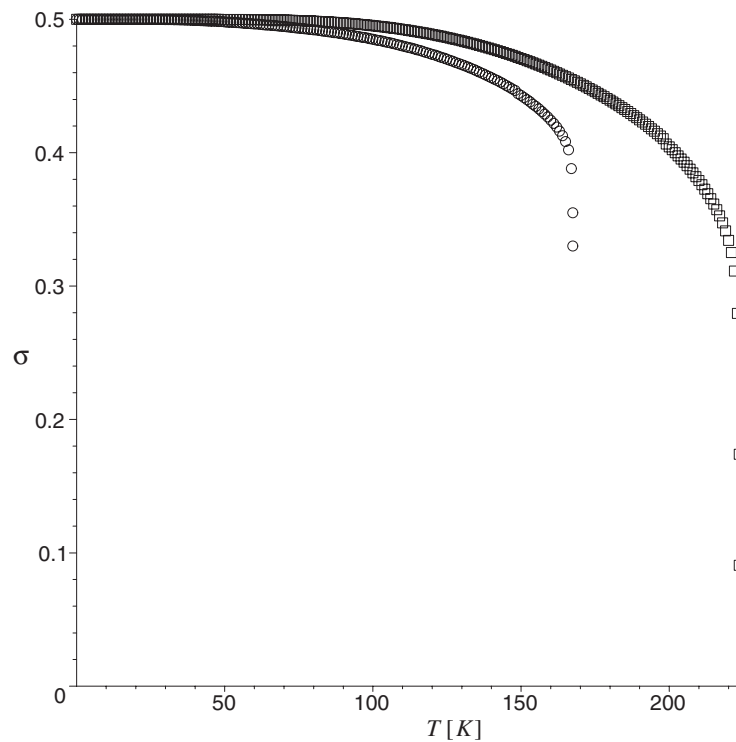


Figure 7. Temperature dependence of the polarization σ with $J_b = 495$ K, $\Omega_b = 20$ K, $J_s = 900$ K, $\Omega_s = \Omega_b$, $N = 9$ and an antiferroelectric defect layer: (1) $J_d = 1000$ K, $T_c = 223$ K (\square), (2) -1000 K, $T_c = 168$ K (\circ).

the substitution of rare earth cations of La, Ce, Pr, Nd and Sm as well as Bi at the A site (Sr site) with Sr vacancies and have shown that La modification induces soft behaviour (lower E_c and lower σ_r), while a large amount of Nd and Sm substitution results in a very high E_c (hard), as a result of defect engineering of both Sr and oxide vacancies. For not only SBT, but also other bismuth layer-structured FEs (BLSFs), T_C is strongly influenced by the r_i of A-site cations, and BLSFs with smaller A-site cations (Ca^{2+}) tend to show a higher T_C (420 °C). The same amount of the larger Ba^{2+} brings about a relaxation of FE distortions and resulted in a decrease in T_C to 120 °C. The substitution of La led to a marked decrease in T_C to 180 °C ($x = 0.5$), because the induced A-site vacancies weaken the coupling between neighbouring BO_6 octahedra [12, 21]. This result corresponds in our calculations to the case of smaller values of the interaction constant in the defect layer $J_d < J_b$. For La-modified PbTiO_3 , T_C decreased significantly, too, with an increase in La content [39]. For Bi-SBT T_C rose strongly to 405 °C ($x = 0.2$) [21]. The increase in T_C with Bi substitution is an opposite tendency to that in the case for La-SBT. The bonding characteristics with oxide ions play the dominant role here. The influence of the orbital hybridization on T_C is very large, and Bi substitution resulted in a higher T_C [21]. This experimental result can be described qualitatively well using in our model exchange interaction parameters for the defect layer $J_d > J_b$.

In figures 3 and 4 is shown the influence of the surface exchange interaction constant J_s on the polarization and spin-wave energy by $J_4 = J_d = \text{const}$ for a thin film with $N = 7$ layers. It can be seen that the two quantities are enhanced with increasing J_s . The critical temperature T_C increases, too.

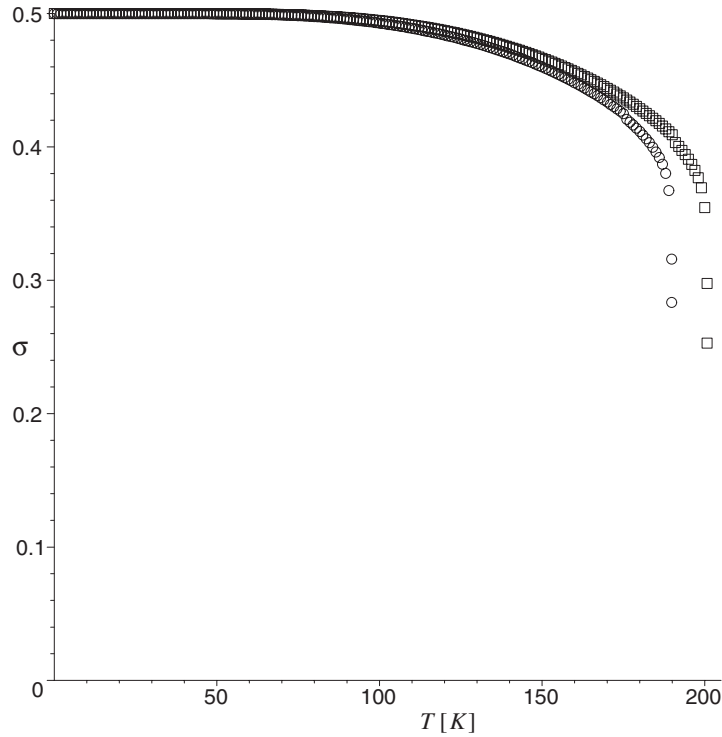


Figure 8. Temperature dependence of the polarization σ with $J_b = 495$ K, $\Omega_b = 20$ K, $J_s = 900$ K, $\Omega_s = \Omega_b$, $N = 9$ and an antiferroelectric defect layer: (1) $J_d = 300$ K, $T_c = 201$ K (\square), (2) -300 K, $T_c = 190$ K (\circ).

The polarization is dependent, too, on how many inner layers are defected. This is shown in figures 5 and 6 for a thin film with $N = 7$ layers. In figure 5 it is demonstrated that for $J_d = 200$ K with increasing number of defect layers (curve 1— $J_4 = J_d = J_b$, curve 2— $J_4 = J_d = 200$ K, curve 3— $J_3 = J_4 = J_5 = J_d = 200$ K) the polarization and the critical temperature decrease. The opposite behaviour can be seen in figure 6, where $J_d = 1000$ K. With increasing of the number of defect layers the polarization and T_C increase. The spin-wave energies are reduced in the first case and enhanced in the second case.

We have also studied thin films with $N = 9$ layers where one layer with defects exhibits an antiferroelectric coupling. Such an antiferroelectric coupling is characterized by a negative parameter J in equation (1). In figure 7, curve 2, we have chosen the parameter $J_5 = J_d = -1000$ K while in figure 8 (curve 2) we have taken $J_5 = J_d = -300$ K. The polarization and T_C of the film are smaller in comparison to the case where the middle layer is a defect one, but with ferroelectric order. The spin-wave energy of the thin film is also reduced when $J_5 = J_d = -1000$ K. Such a sublattice model with ferroelectric and antiferroelectric layers where one or more layers are defected will be studied in a forthcoming paper.

4. Conclusions

In conclusion, based on a modified transverse Ising model and using a Green function technique, the polarization, the spin-wave energies and the phase transition temperature for ferroelectric thin films with structural defects are calculated. The dependence on temperature, film thickness

and interaction constants is discussed. It is shown that defect layers in FE thin films, layers with impurities or vacancies or with dislocations, can induce a strong increase or decrease of the polarization, the spin-wave energies and the critical temperature of FE phase transition due to different exchange interactions in the defect layers. The results are in good agreement with the experimental data for different ferroelectrics. In particular, our results are also in accordance with recent theoretic studies based on a generalized Ginzburg–Landau model [34, 35] and some experiments [36, 37].

Acknowledgments

One of us (JMW) is grateful to the Deutsche Forschungsgemeinschaft for financial support. This work is supported by the SFB 418. Further, we thank Dr D Hesse and Dr M Alexe, Max Planck Institute of Microstructure Physics, Halle, for fruitful and exciting discussions on experimental details.

References

- [1] Grenier J C, Schiffmacher G, Caro P, Pouchard M and Hagemuller P 1977 *J. Solid State Chem.* **20** 365
- [2] Beccero A I, McCammon C A, Langenhorst F, Seifert F and Angel R J 1999 *Phase Transit.* **69** 133
- [3] Steinsvik S, Bugge R, Gjønnes J, Taftø J and Norby T 1997 *J. Phys. Chem. Solids* **58** 969
- [4] Dawber M and Scott J F 2000 *Appl. Phys. Lett.* **76** 1060
- [5] Scott J F 2001 *Integr. Ferroelectr.* **32** 951
Scott J F 2001 *Integr. Ferroelectr.* **38** 125
- [6] Stemmler S 1995 *Phil. Mag. A* **71** 713
- [7] Scott J F 2000 *Ferroelectric Memories* (Berlin: Springer)
- [8] Kim S H, Yang J S, Koo C Y, Yeom J H, Yoon E, Hwang C S, Park J S, Kang S G, Kim D J and Ha J 2003 *Japan. J. Appl. Phys.* **42** 5952
- [9] Tohma T, Masumoto H and Goto T 2003 *Japan. J. Appl. Phys.* **42** 6969
- [10] Pontes F M, Leal S H, Leite E R, Longo E, Pizani P S, Chiquito A J and Varela J A 2004 *J. Appl. Phys.* **96** 1192
- [11] Chu M W, Szafraniak I, Scholz R, Harnagea C, Hesse D, Alexe M and Goesele U 2004 *Nat. Mater.* **3** 87
- [12] Sakai T, Watanabe T, Funakubo H, Sarro K and Osada M 2003 *Japan. J. Appl. Phys.* **42** 166
- [13] Kim J S, Kim S S and Kim J K 2003 *Japan. J. Appl. Phys.* **42** 6486
- [14] Choi E K, Kim S S, Kim J K, Bae J C, Kim W J, Lee Y J and Song T K 2004 *Japan. J. Appl. Phys.* **43** 237
- [15] Watanabe T, Kojima T, Uchida H, Okada I and Funakubo H 2003 *Japan. J. Appl. Phys.* **43** L309
- [16] Noguchi Y, Miyayama M, Oikawa K, Kamiyama T, Osada M and Kakihana M 2002 *Japan. J. Appl. Phys.* **41** 7062
- [17] Aizawa K and Ishiware H 2003 *Japan. J. Appl. Phys.* **42** L840
- [18] Das R R, Bhattacharya P, Perez W and Katiyar R S 2003 *Japan. J. Appl. Phys.* **42** 162
- [19] Berlincourt D, Curran D and Jaffe H 1964 *Physical Acoustics* vol 1, ed W Cady (New York: Academic)
- [20] Shimakawa Y and Kubo Y 1999 *Appl. Phys. Lett.* **74** 1904
- [21] Noguchi Y, Miyayama M and Kudo T 2001 *Phys. Rev. B* **63** 214102
- [22] Robins L H, Kaiser D L, Rotter L D, Schenck P K, Stauff G T and Rytz D 1984 *J. Appl. Phys.* **76** 7487
- [23] Tenne D A *et al* 2004 *Phys. Rev. B* **69** 174101
- [24] Donnelly D, Hone D and Jaccarino V 1990 *Phys. Rev. Lett.* **65** 2286
- [25] Costa Filho R N, Costa U M S and Cottam M G 2000 *J. Magn. Magn. Mater.* **213** 195
- [26] Wesselinowa J M 2001 *Phys. Status Solidi b* **223** 737
- [27] Pantic M, Manojlovic M, Skrinjar M, Pavkov M, Kapor D and Stojanovic S 2004 *Int. J. Mod. Phys. B* **18** 1537
- [28] Zhang X L, Gu B Y and Chen K Q 2003 *Phys. Lett. A* **316** 107
- [29] Vikhin V S and Maksimova T I 2004 *Ferroelectrics* **299** 43
- [30] Dieguez O, Tinte S, Antons A, Bungaro C, Neaton J B, Rabe K M and Vanderbilt D 2004 *Phys. Rev. B* **69** 212101
- [31] Pertsev N A, Zembilgotov A G and Tagantsev A K 1998 *Phys. Rev. Lett.* **80** 1988
- [32] Alpaya S P, Misirlioglu I B, Sharma A and Ban Z G 2004 *J. Appl. Phys.* **95** 8118
- [33] Alpaya S P, Misirlioglu I B, Nagarajan V and Ramesh R 2004 *Appl. Phys. Lett.* **85** 2044

- [34] Catalan G, Sinnamon L J and Gregg J M 2004 *J. Phys.: Condens. Matter* **16** 2253
- [35] Bratkovsky A M and Levanyuk A P 2005 *Phys. Rev. Lett.* **94** 107601
- [36] Lookman A, Bowman R M, Gregg J M, Kut J, Rios S, Dawber M, Ruediger A and Scott J F 2004 *J. Appl. Phys.* **96** 555
- [37] Saad M M, Baxter P, Bowman R M, Gregg J M, Morrison F D and Scott J F 2004 *J. Phys.: Condens. Matter* **16** L451
- [38] Lai B K, Kornev I A, Bellaiche L and Salano G J 2005 *Appl. Phys. Lett.* **86** 132904
- [39] Kim T Y and Jang H M 2000 *Appl. Phys. Lett.* **77** 3824